Methodologies for Coupled Transient Electromagnetic-Thermal Finite Element Modeling of Electrical Energy Transducers

Johan Driesen, Ronnie Belmans and Kay Hameyer

KATHOLIEKE UNIVERSITEIT LEUVEN, DEP. EE (ESAT), DIV. ELEN

Kardinaal Mercierlaan 94, B-3001 Leuven, BELGIUM

Abstract — **The coupled transient computation of the interacting electromagnetic-thermal fields in electrical energy transducers containing significantly different time constants is discussed. Methodologies to deal with the numerical stiffness, encountered in the magnetic field, thermal field and loss computation, while using standard integration methods, are outlined. Such computation techniques are illustrated using two application examples: a permanent magnet synchronous machine and a three-phase transformer.**

Index Terms — **electro-thermal effects, finite element method, thermal modeling**

I. INTRODUCTION

A. Problem Situation

In different types of electrical energy transducers such as transformers, electrical machines and generators, it is important to study the electromagnetic behavior jointly with the thermal behavior, for instance to study the efficiency, to estimate the life-time, etc. Two interactions justify such a coupled view:

- Most thermal energy sources heating up these devices are in fact electromagnetic losses. These can be Joule type losses such as eddy current losses or iron losses. Generally, these quantities are a function of the local electromagnetic field. Therefore they represent a coupling of the electromagnetic field to the thermal field.

- Many material characteristics playing a role in the electromagnetic field are depending on the local temperature. For instance, the electrical conductivity of a copper conductor may change about 30 % over the temperature interval of some 100 °C in which most electrical machines operate. Another important example is the shift of the permanent magnet characteristic of the

hard magnetic materials involved in permanent magnet machines under local temperature changes [1].

For these reasons, it is often a necessity to perform a coupled field analysis, using for instance the Finite Element Method (FEM) [2], already in the design stage of the electrical energy transducer. However, the different nature of the physical fields involved and especially the dynamics, reflected in their characteristic time constants, impose difficulties in the simulation.

B. Numerical Stiffness

Transient numerical simulations become troublesome when the system to be simulated contains dynamic phenomena on a largely different time scale (time constant) [3]. In the case of electromagnetic fields, the typical time scale is small as it is governed by the supply's fundamental frequency and the rotation. It can even be smaller when power electronic supplies using PWM techniques, yielding enlarged losses, are used. On the other hand, the thermal field changes at a much slower rate. The ratio between the largest and smallest time constant is known as the stiffness ratio, which can have values of as high as 10^{10} for electrical machines.

The mathematical difficulty arising while simulating the coupled transient behavior is known as numerical stiffness. Other authors dealing with similar and other coupled problem computations (e.g. [4]) encountered similar problems and used adapted techniques such as backward differentiation (BDF) methods. This problem is treated in this paper along with some approaches to solve it while using standard integration methods.

The main problem is related to the time step choice in the simulation. The following options exist:

- the choice of a very small but stable time step, related to the magnetic field dynamics, yielding an extremely long calculation time;

- the choice of a large time step related to the thermal time step, requiring special, expensive integration methods in order to obtain a stable computation;

- it might seem interesting to use different time steps for the subproblems, but this involves a possibly unstable extrapolation;

- assume that one of the subproblems is in a 'continuous steady-state': this technique is often applied (e.g. [5]), more in particular when the magnetic field is recalculated

in the frequency domain after every time step, however, it cannot be excluded that the underlying implicit extrapolation yields a divergence as demonstrated in [6];

- adapt the problem formulation to work around a time scale and use standard integration methods.

The latter approach is illustrated here.

II. MAGNETIC FIELD ANALYSIS

The 2D magnetic field equation is written in terms of the magnetic vector potential [7]:

$$\nabla \cdot (\upsilon(A(t))\nabla(A(t))) = -\sigma(T(t))\left(V_s(t) + \frac{dA(t)}{dt}\right) - \nabla M(T(t)) \quad (1)$$

with: A : z-component of the vector potential
T : Temperature
υ : Reluctivity
σ : Electrical conductivity
V_s: Source voltage
M : Permanent magnet source field

In the further development of this equation, one has to account for the rotational time constant. Two approaches are made, depending on the preferred choice of reference frame.

A. Reference frame with fixed magnetic field

In electrical machines such as *DC*-machines and synchronous machines, it is interesting to fix the reference frame to the field source to obtain a relatively fixed magnetic field arrangement. For synchronous machines, it is fixed to the rotor and for *DC*-machines to the stator. In that case, the induced voltage term is developed as:

$$\sigma(t)\frac{dA}{dt} = \sigma(t)\left(\frac{\partial A}{\partial t} + \vec{v} \cdot \nabla A\right) \quad (2)$$

For a rotating device, the effect of the second term in (2) containing the speed $\vec{v}$, representing the voltage induced by the rotation, is dominant over the local field changes described by the first term. However, these changes contribute to the losses (e.g. in the magnets). The first term in (2) is neglected in the global field calculation, the second term is usually calculated separately, by extracting the fundamental induced voltage [8]. It is then substituted in (1) as a finite difference (3). The parameter θ originates from the time stepping method [7].

$$\begin{aligned}\sigma(t)\frac{dA}{dt} &\approx \sigma(t)(v(t) \cdot \nabla A) \\ &\approx \theta\sigma(t_{n+1})v(t_{n+1}) \cdot \nabla A(t_{n+1}) + (1-\theta)\sigma(t_n)v(t_n) \cdot \nabla A(t_n)\end{aligned} \quad (3)$$

Consequently, the magnetic model is reduced to a series of (semi-)static magnetic field computations with externally determined currents, computed once per thermal time-step.

The temperature dependent material properties change with the pace of the thermal model's time-step.

B. Reference frame with rotating or oscillating magnetic field

Alternatively, it is possible to use a reference frame in which the magnetic field rotates or oscillates, for instance in an induction machine or in a transformer. An efficient transient-type solver can still be obtained by assuming the solution can be written in the following complex form, with ω the field pulsation [6]:

$$A(t) = \underline{A}(t) \cdot e^{j\omega t} \quad (4)$$

This is an extension of the assumption behind the time-harmonic method [7], but now we assume the solution part in the complex phasor form changes in time. Eq. (4) splits the fast dynamics at the studied frequency (the exponential terms) and the slow dynamics in the phasor. The phasor can be interpreted as complex 'envelope' of the fast oscillating harmonic function (Fig. 1).
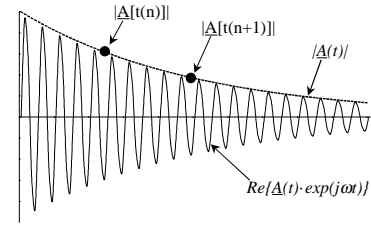

Fig. 1. A function with fast (oscillation) and slow dynamics (envelope evolution). The function envelope evolution is to be simulated.

Assuming the source in (1) is written in the form of (4) and neglecting the permanent magnetisation, this leads to:

$$\nabla \cdot (\upsilon \nabla(\underline{A})) - \sigma(T)\left(j\omega \underline{A} + \frac{\partial \underline{A}}{\partial t}\right) = -\sigma(T)\underline{V} \quad (5)$$

This equation is transformed into FEM equations using the Galerkin method. The time derivative is replaced by a finite difference with the Δt of the thermal equation:

III. THERMAL FIELD ANALYSIS

Although the thermal field calculation seems more or less obvious, the rotation has to be dealt with as well. This reflects in the spatial distribution of the losses and the different radial heat paths. To get around this problem, one can use two models using different reference frames. One model uses a stator-fixed frame, while the other uses a rotor-fixed frame (see [9] for the background of this methodology). The thermal field equation is:

$$\nabla \cdot (k\nabla(T)) - \rho c \frac{\partial T}{\partial t} = -q(A,T) \quad (6)$$

with: T : Temperature

q :	Total losses
k :	Thermal conductivity
ρ :	Mass density
c :	Specific heat

To model the cooling, these models are extended with convective boundary conditions. Air gaps are generally represented by means of an equivalent heat-conducting material. The equivalent conductivity is calculated considering the thermal resistance obtained by applying two convective transfers in series. The convective heat coefficients are calculated considering the state of the air flow in the air gap. Convection parameters for the inner parts are difficult to determine. Equivalent anisotropic materials or special element relations are used to model thermal contact resistances and thin insulation layers [9].

IV. FIELD INTERACTIONS

A. Thermally dependent material characteristics

Generally, for the temperature range in which the majority of electrical machines operate, two types of thermally dependent material characteristics have to be taken into account:

- *electrical conductivity* : within the finite element, the value is updated using the temperature change and the thermal coefficient.
- *permanent magnet characteristic* : the shift of the characteristic is used to implement the change of the magnetization in (1). The point of irreversible magnetization alters as well.

B. Loss calculations

Several types of losses are to be included in the right-hand side term of the thermal equation, each with a different specific calculation method:

- *Joule losses* : This loss density is computed by calculating the joule loss integral in every conductor finite element. Eddy current contributions may be present.
- *Iron losses* : These have different components (hysteresis, eddy current and excess losses) and are calculated by numerically integrating, for every finite element, analytical expressions using the field changes during one rotation [11]. These values are calculated based on the flux loci in the elements (Fig. 2), obtained from the set of semi-static magnetic models, each rotated over a small angle (Fig. 3). These FEM calculations are performed relatively fast, since the saturation can be 'frozen' yielding a linear problem. Hence, fast rotational effects are counted in.
- *Permanent magnet Joule losses* : These occur in electrically conductive surface mounted permanent magnet blocks and are calculated under the simplifying assumption that they do not affect the global magnetic

field, so the first term in (2) can be reconstructed in the permanent magnet finite elements, based on the same set of semi-static magnetic models at consecutive rotation angles [12], already made for the iron loss calculation. This approach takes into account the higher field harmonics on the smallest time scale.
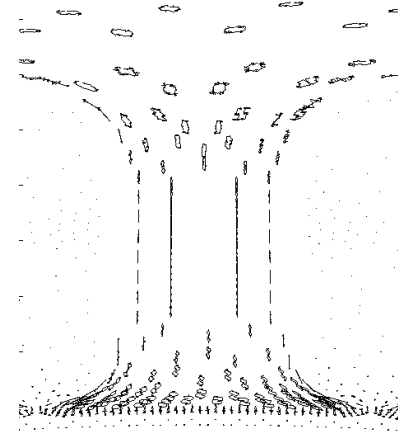
Fig. 2. Reconstructed trajectories (loci) of the endpoints of the magnetic field vector in different locations in a tooth of a partially loaded PMSM.
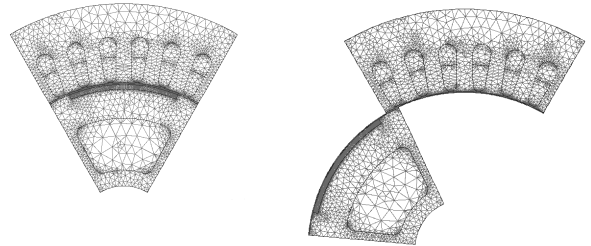
Fig. 3. Two meshes used in the procedure to calculate the iron and permanent magnet eddy current losses.

IV. COUPLED SIMULATION

The actual calculation of the coupled field problem is best computed using 'block iteration' algorithms (Fig. 4).
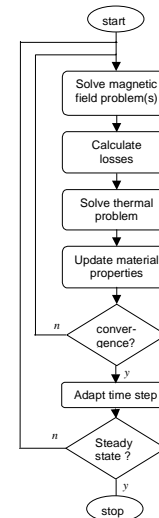
Fig. 4. Coupled problem computation flow chart.

These are preferable over Newton-type methodologies [13] as Newton algorithms require the knowledge of all time derivatives, which cannot be easily expressed, and the obtained matrix systems to be solved are asymmetric and ill-conditioned and therefore require expensive solver algorithms.

V. APPLICATIONS

To illustrate the methodologies described above, two examples are included. At first, a permanent magnet synchronous machine is calculated using a fixed reference frame for the magnetic field calculation [14]. Secondly, the approach for the oscillating or rotating *AC* fields is demonstrated for a three-phase transformer [15].

A. Permanent Magnet Synchronous Machine

To study the dynamic performance of a 45 kW 6-pole PMSM designed for use in an electrical vehicle, a transient coupled thermal magnetic simulation is developed. This machine is designed to have a water cooling system and contains conductive, temperature sensitive NdFeB permanent magnet pieces fixed to the rotor surface. The mesh used for the magnetic field calculation is shown in Fig. 3. Fig. 5 represents the magnetic field.
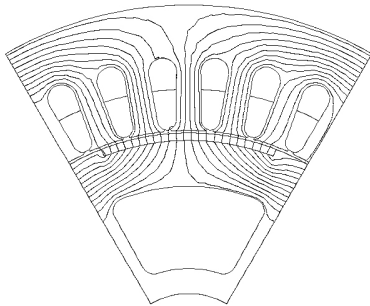
Fig. 5. Magnetic field solution of the PMSM in loaded conditions.

Two thermal models, with stator and rotor reference frame are used in the thermal calculation (Fig. 6). They contain appropriate contact resistance and insulation representations. The air gap convection parameter is determined using semi-empirical correlations. The losses were determined using the method described above.
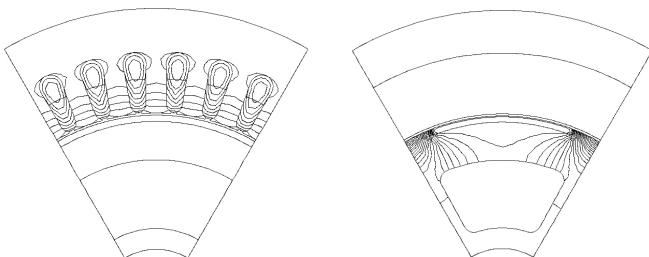
Fig. 6 PMSM thermal solution - stator and rotor frame model; used to update the winding electrical conductivity permanent magnet data.

To validate the coupled model, it was tested in different circumstances. In a first test, the machine is used as a water-cooled generator driven by a *DC*-motor at 1500 rpm. Its winding is connected to a resistive load. All types of losses are considered in the motor. The iron losses drop about 20 % when the iron gets hot and the permanent magnet induced flux is weakened. The joule losses in the winding rise about 19 % due the heating. Measured temperatures are compared to computed values (Fig. 7).
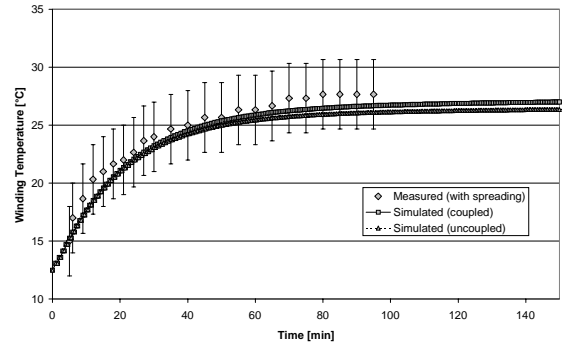
Fig. 7. Comparison of measured and calculated winding temperature variations in water-cooled loaded conditions (the variance coming from redundant sensors is indicated).

In this graph, a good agreement between measured and simulated data is found. The results of an uncoupled calculation are plotted as well, these are situated below the coupled result, since the increased resistivity is not taken into account, which introduces a systematic underestimation of the losses. The variance between the coupled and uncoupled simulation is not very large, though it represents a difference of about 4.4 % for this limited temperature rise of merely 15 °C.

In a no-load test, the PMSM is driven by the *DC*-motor at 3000 rpm. The windings are open and the induced voltage is measured. The water cooling is inactive. In this case, only iron losses are present. The evolution of the registered temperatures, along with the simulations is shown in Fig. 8. The variation of the fundamental measured and induced voltage is given in Fig. 9.
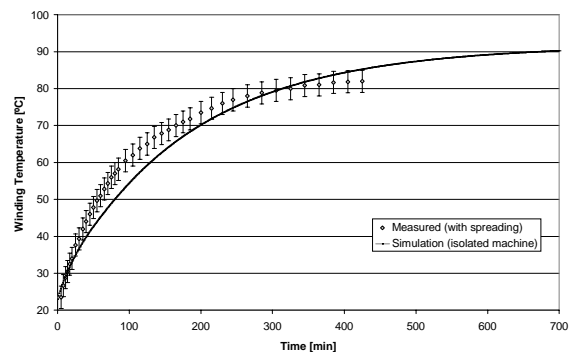
Fig. 8. Comparison between simulated and measured temperatures in air-cooled unloaded conditions (the variance in the measured values is indicated).
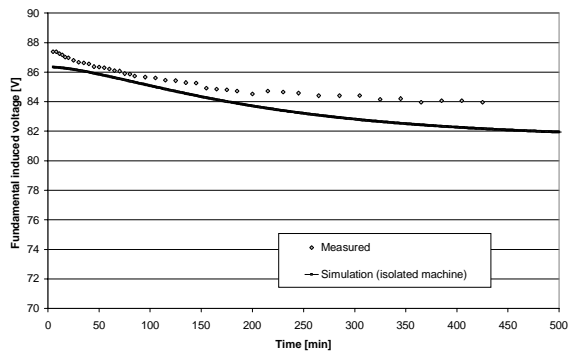
Fig. 9. Comparison of fundamental measured and induced voltage.

The first graph indicates that the computed steady-state temperature of the device is about 5 % higher than measured. An explanation is found in the fact that some parasitic heat paths are neglected. Neither the heat flux through the mounting (the motor is not perfectly insulated from the base plate on the test bench), nor the heat flowing out of the motor through the rotating shaft is taken into account. A test calculation indicates that the temperature drops to the measured level, when it is assumed that these conductive phenomena increase the cooling capability by 10 %. For the measurements, the stator temperature rises a bit faster in the beginning. This is due to the convection cooling models used, becoming more accurate when the temperature differences are more significant. The induced voltage follows the measured value, which is an indirect measure of the magnet temperature. An average change of more than 5 % of the magnets' remanent field is found.

B. Three-Phase Transformer

A 30 kVA transformer having 50 foil conductors in the secondary winding, which are located close to the core, is modelled in the described way. The meshes are constructed by using adaptive refinement techniques. The real component of the magnetic solution of the simulated short-circuit test is shown in Fig. 10. Fig. 11(a) shows a detail of the leakage field.
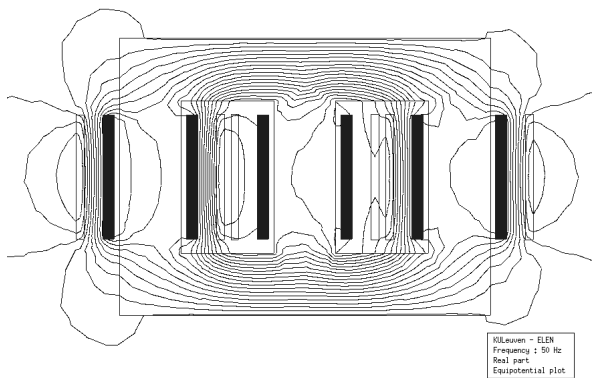

Fig. 10. Real part of the final magnetic field solution of a simulated short circuit test.

The surrounding air and the air between the winding blocks is replaced by convective boundary conditions. The thermal mesh is extended with thin layer elements between the foils, representing the insulation layers and anisotropic materials. A detail of the thermal solution is shown in Fig. 11(b), clearly indicating the location of the hot spot in the top of the foil winding coil.
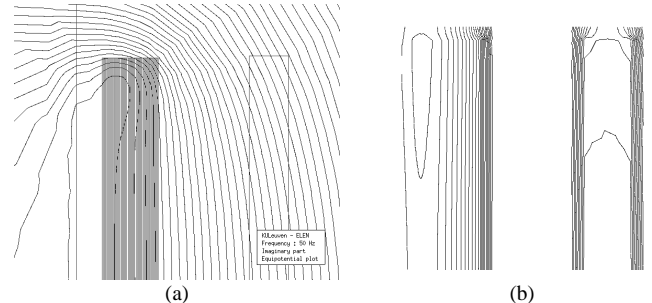

(a)   (b)

Fig. 11: Details of the magnetic and thermal field. (a) field lines of the leakage flux passing through the foil conductors in the top the coil associated with additional eddy currents; (b) Isothermal lines of the upper part of a coil set; on the left the foil conductor; on the right the wire coil; hot spot is visible in the top of the foil pack.

To validate the transient method, measurements were made and compared with simulations. Fig. 12 demonstrates that there is a good correspondence. The difference between the steady state temperature in the measurements and the simulation, as well as the small difference in the thermal heating time constant, are explained by the difficulty to model the natural convective cooling in the vicinity of the coils.
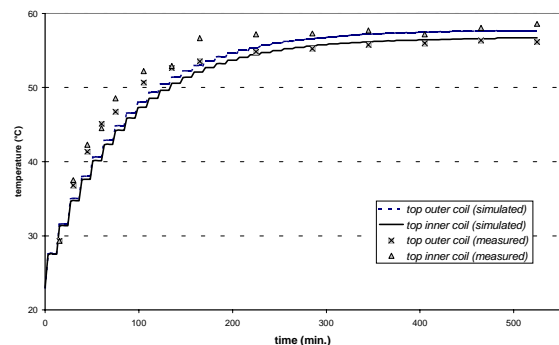

Fig. 12. Comparison of measured and calculated heating of the transformer in a short circuit situation. The temperature near the tops on the outer side is measured optically.

CONCLUSIONS

This paper discusses manners to deal with the large difference in time scales encountered in the simulation of coupled electromagnetic-thermal field problems in electrical energy transducers. The high ratio between the largest and smallest time constants yields numerical stiffness, which would normally require special integration methods.

However, by reworking some of the problem modeling aspects it is possible to separate some of the dynamic phenomena at different time scales. In this way it becomes possible to split up rotation or oscillation, higher-order harmonics generating losses and the heating up of the device.

To illustrate these methodologies, the transient thermal-magnetic computation of a permanent magnet synchronous machine and a three-phase transformer is discussed and compared with measurements.

REFERENCES

[1] E.S.Hamdi, *Design of Small Electrical Machines,* J.Wiley & Sons, Chichester-New York-Singapore, 1994.

[2] O.C.Zienkiewicz, R.L.Taylor, *The finite element method*, 4th ed., Vol. 1, Basic formulation and linear problems, McGraw-Hill Book Company, 1994.

[3] W.L.Willard, *Numerical methods for stiff equations and singular perturbation problems*, D.Reidel Publishing Company, 1981.

[4] N.A.Demerdash, J.F.Bangura, A.A.Arkadan, "A Time-Stepping Coupled Finite Element-State Space Model for Induction Motor Drives, Part 1: Model Formulation and Machine Parameter Computation," *IEEE Trans. on Energy Conversion*, Dec.'99, Vol.14, No.4, pp.1465-1471.

[5] J.Xypteras, V.Hatziathanassiou, "Transient thermal field of a squirrel cage motor with deep-bar effect," Proc. Int. Conf. On Electrical Machines (ICEM '94), Paris, France, pp.429-433.

[6] J.Driesen, K.Hameyer, "The simulation of magnetic problems with combined fast and slow dynamics using a transient time-harmonic method," 3ième conférence Européenne sur les méthodes numériques en electromagnétisme (NUMELEC), Poitiers, France, Mars 20-22.2000, pp.166-167.

[7] K.J.Binns, P.J.Lawreson, C.W.Trowbridge, *The Analytical and Numerical Solution of Electric and Magnetic Fields*, Wiley, 1992.

[8] U.Pahner, S.Van Haute, R.Belmans, K.Hameyer, "Comparison of two methods to determine the d/q-axis lumped parameters of permanent magnet machines with respect to numerical optimisation," Proc. Int. Conf. On Electrical Machines (ICEM '98), Istanbul, Turkey, 2-4 Sept. 1998, pp.352-357.

[9] J.Driesen, R.Belmans, K.Hameyer, "Coupled magneto-thermal simulation of thermally anisotropic electrical machines," IEEE International Electric Machines and Drives Conference (IEMDC'99), Seattle, Washington, USA, 9-12.05.99, pp.469-471.

[10] J.Driesen, R.Belmans, K.Hameyer, "Finite element modelling of thermal contact resistances and insulation layers in electrical machines," accepted for publication in *IEEE Trans. on Industry Applications*.

[11] Z. Liu, D. Howe, P. Mellor, M. Jenkins: "Coupled thermal and electromagnetic analysis of a permanent magnet brushless DC servo motor," Proc. IEE Int. Conf. on Electrical Machines and Drives '93, 8-10 September 1993, Oxford, UK, pp. 631-635.

[12] N. Schofield, K. Ng, Z. Zhu, D. Howe: "Parasitic rotor losses in a brushless permanent magnet traction machine," Proc. IEE Int. Conf. on Electrical Machines and Drives '97, 1-3 September 1997, Cambridge, UK, pp.200-204.

[13] J.Driesen, K.Hameyer, "Comparison of strong and weak coupled solution algorithms for coupled electromagnetic-thermal problems," 9th Biennial IEEE conf. on electromagnetic field computation – CEFC 2000, Milwaukee-Wisconsin, USA, June 4-7.2000, p.87.

[14] J.Driesen, U.Pahner, R.Belmans, K.Hameyer, "Transient coupled magnetic thermal analysis of a permanent magnet synchronous electrical vehicle motor," Proc. Int. Conf. on Electrical Machines (ICEM 2000), Espoo, Finland, August 28-30.2000, Vol.1, pp.343-347.

[15] J.Driesen, G.Deliège, K.Hameyer, "Coupled thermo-magnetic simulation of a foil-winding transformer connected to a non-linear load," 12th Conf. on the Computation of Electromagnetic Fields (COMPUMAG '99), Sapporo, Japan, 25-28 October 1999, Vol.2, PF2-5, pp.588-589.

Johan Driesen (S'93-M'97) graduated in 1996 as Electrotechnical Engineer from the Katholieke Universiteit Leuven (KULeuven). Since 1996 he was a research assistant of the Fund for Scientific Research of Flanders (F.W.O.-Vl.). He received the 1996 R&D-award of the Belgian Royal Society of Electrotechnical Engineers (KBVE) for his Master Thesis on power quality problems. He received the Ph.D. degree in Electrical Engineering at K.U.Leuven in 2000 on the finite element solution of coupled thermal-electromagnetic problems and related applications in electrical machines and drives, microsystems and power quality issues. Currently he is a postdoctoral research fellow of the Belgian "Fonds voor Wetenschappelijk Onderzoek - Vlaanderen".

Kay Hameyer (M'95) received the M.S. degree in electrical engineering in 1986 from University of Hannover, Germany. He received the Ph.D. degree from University of Technology Berlin, Germany, 1992.

From 1986 to 1988 he worked with the Robert Bosch GmbH in Stuttgart, Germany, as a design engineer for permanent magnet servo motors. In 1988 he became a member of the staff at the University of Technology Berlin, Germany. From November to December 1992 he was a visiting professor at the COPPE Universidade Fderal do Rio de Janeiro, Brazil, teaching electrical machine design. In the frame of a collaboration with the TU Berlin, he was in June 1993 a visiting professor at the Université de Batna, Algeria. Beginning in 1993 he was a scientific consultant working on several industrial projects. From 1993 to March 1994, he held a HCM-CEAM fellowship financed by the European Community at the Katholieke Universiteit Leuven, Belgium. Currently he is professor for numerical field computations and electrical machines with the K.U.Leuven and a senior researcher with the F.W.O.-V. in Belgium, teaching CAE in electrical engineering and electrical machines. His research interests are numerical field computation, the design of electrical machines, in particular permanent magnet excited machines, induction machines and numerical optimization strategies.

Dr. Hameyer is member of the International Compumag Society and the IEEE.

Ronnie J.M.Belmans (S'77-M'84-SM'89) received the M.S. degree in electrical engineering in 1979 and the Ph.D. in 1984, both from the Katholieke Universiteit Leuven, Belgium, the special Doctorate in 1989 and the Habilitierung in 1993, both from the RWTH Aachen, Germany.

Currently, he is a full professor with the K.U. Leuven, teaching electrical machines, power electronics and variable speed drives. His research interests include power quality, electrical energy systems, electrical machine design and vibrations and audible noises in electrical machines. He was with the Laboratory for Electrical Machines of the RWTH Aachen, Germany, as a Von Humboldt Fellow (October 1988-September 1989). From October 1989 to September 1990, he was visiting professor at the McMaster University, Hamilton, ON., Canada. He obtained the chair of the Anglo-Belgian Society at the London University for the year 1995-1996. Currently he is a visiting professor at Imperial College in London U.K.

Dr. Belmans is a fellow of the IEE (U.K.), the International Compumag Society and the Koninklijke Vlaamse Ingenieursvereniging (KVIV).